

ELECTRON DENSITY VARIATION IN OFF-LIMB SOLAR CORONA STRUCTURES

I. Ugarte-Urra,* J.G. Doyle, and M.S. Madjarska

Armagh Observatory, College Hill, Armagh BT61 9DG, N. Ireland

ABSTRACT

We present a study of the electron density variation for off limb observations with the Coronal Diagnostic Spectrometer (CDS) on board SoHO using the density sensitive coronal line ratio Si X (356.0/347.4). The analysis is divided into three parts: the latitudinal variation from $1.01 < r/R_{\odot} < 1.09$, the temporal variation in successive rasters, and the electron density along a hot coronal loop found in one of the rasters.

Key words: CDS; SoHO; electron density; off limb; latitudinal dependence; coronal loop.

1. INTRODUCTION

In the SoHO era, important efforts have been made to determine the density, temperature and velocity above the solar limb. The importance of these studies comes from the fact that these parameters are essential constraints to the understanding of the solar wind. Recently a MHD model by Lima *et al.* (2001) has made an attempt to predict the latitudinal and radial dependence of the solar wind parameters. In the present paper we present a study of the electron density, N_e , above the solar limb, extending the latitudinal dependence study done in one quadrant of the solar disk by Gallagher *et al.* (1999), to the whole disk. We also show the variation of the electron density for consecutive daily rasters, and with the help of these results we have been able to determine the variation of N_e along a coronal loop observed in one of the rasters (1998 April 6).

2. OBSERVATIONS AND DATA REDUCTION

The observations were made with the Coronal Diagnostic Spectrometer (CDS) on board SOHO between March and April 1998. The rasters cover several positions all around the solar disk (Figure 1) and were obtained over a period of 9 days (March 29 - April 6). Each raster is a result of sixty slit exposures of 90 seconds at adjacent solar

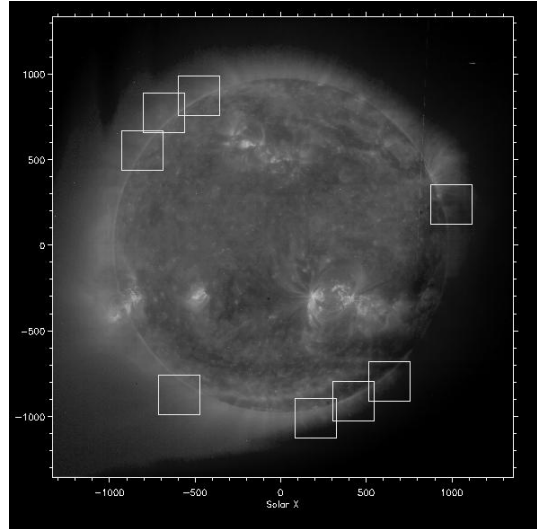


Figure 1. Full disk EIT image (1998 March 29) in Fe IX/X 171 Å with the CDS raster positions overlotted.

X positions. The electron density was determined using the density sensitive line ratio Si X (356.0/347.4) and the CHIANTI atomic database. The lines have a formation temperature of $T_e \sim 1.3 \times 10^6$ K.

3. RESULTS

Three connected studies have been carried out: the latitudinal variation of the electron density all around the solar disk, the temporal variation of the electron density in successive days, and a detailed study of the electron density along a loop.

3.1. Latitudinal variation

In order to improve the signal to noise level we binned spatial pixels “off-chip”, i.e. in the analysis. A binning of 3×7 pixels was used where the X and Y spatial resolution is $4.''064$ and $1.''68$, respectively.

The latitudinal dependence of the electron density for distances $1.01 < r/R_{\odot} < 1.09$ is shown in Figure 2, where

*iuu@star.arm.ac.uk

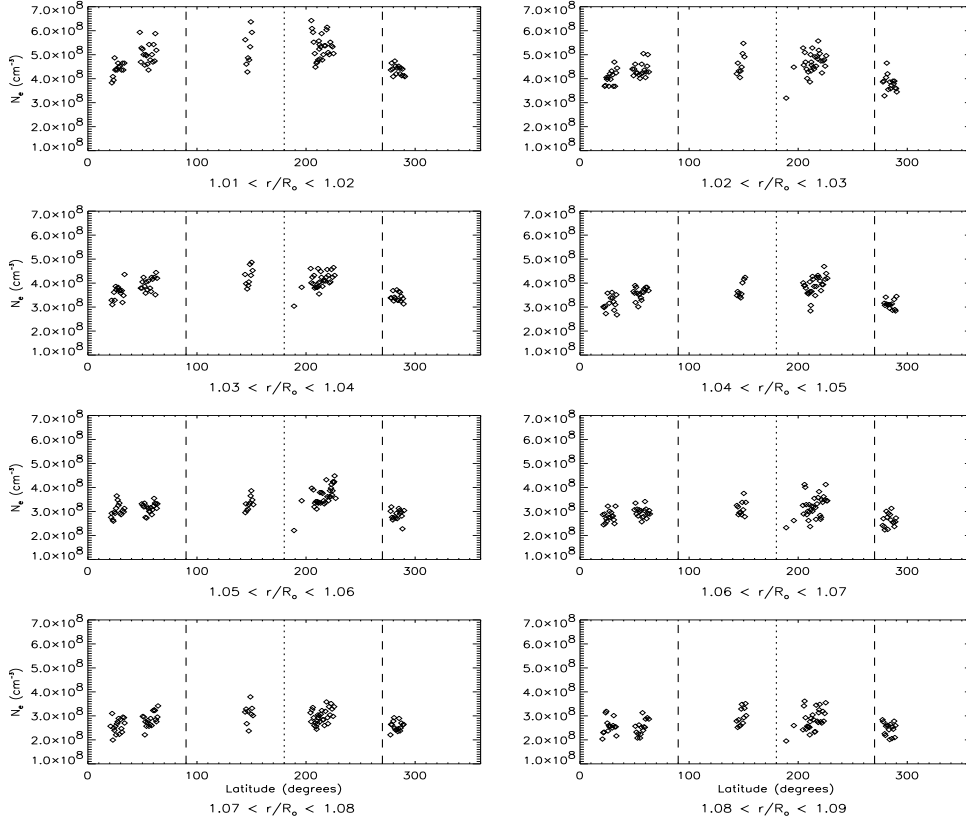


Figure 2. Latitudinal variation of N_e in intervals of $0.01 R_\odot$ (solar radius). 0° corresponds to the north pole and 90° to the east limb.

0° corresponds to the north pole and 90° to the east limb.

A general trend of increasing electron density is seen from the poles towards the equators in the first (0 - 90°) and third (180 - 270°) quadrants. The same trend but decreasing is expected in the other two. The points in the fourth quadrant have lower densities than predicted. The uncertainty for the values of the electron density is in the range 10-40%, increasing with radial distance.

This behaviour has already been observed previously for one quadrant (Gallagher *et al.*, 1999) and predicted by the model of Lima & Priest (1993). We intend to apply the MHD wind model with latitudinal dependences developed by Lima *et al.* (2001), into this data.

3.2. Temporal variation

We used rasters of different days with the same pointing to study the radial decay of the electron density and its variation in successive days over quiet Sun conditions.

We found that the electron density remains constant, within our error bars, at the same location off limb in the period of one day, as can be seen in two radial profiles shown in Figure 5, for two different pointings. We avoided active regions and prominences, since the electron density became clearly higher and lower, respectively, than the value over quiet Sun.

3.3. Coronal loop

In one of the rasters, a coronal loop is clearly visible in the hot line Fe XVI 360.7 \AA ($T_e \sim 2.5 \times 10^6 \text{ K}$), (Figure 3a). As we go to cooler lines, like Si XII or Al XI ($T_e \sim 1.5 - 2 \times 10^6 \text{ K}$), the apex of the loop becomes fainter and appears as a loop not completely closed. The lines with formation temperature of $T_e \sim 1.3 \times 10^6 \text{ K}$ (Si X, Fe XIII) are bright only at the legs and footpoints and for the coolest lines of the raster (Mg IX and Mg X, $T_e \sim 1.0 \times 10^6$) only the footpoints are visible.

We studied N_e along the loop dividing its structure in 17 sections of ~ 20 pixels (Figure 3d) in order to get enough signal, using as a proxy the shape given by the image in Fe XVI (Figure 3a). Then we compared the value of N_e in these sections (black circles in Figure 4) to the value obtained the previous day, in a quiet sun image, at the same angular and radial positions (open circles). As previously mentioned, these values should be the same for both days if the loop was not present, so the difference would be due uniquely to the presence of the loop. We also used two radial profiles outside the loop (Figures 3b and 3d) that confirmed that assumption (asterisks and black triangles). In the case of these two profiles, we had to discard the first three sections for the one on the left and the first section for the one on the right because of a bad row of pixels on the image.

In order to remove the electron density background contribution to the loop, we fitted the four profiles described

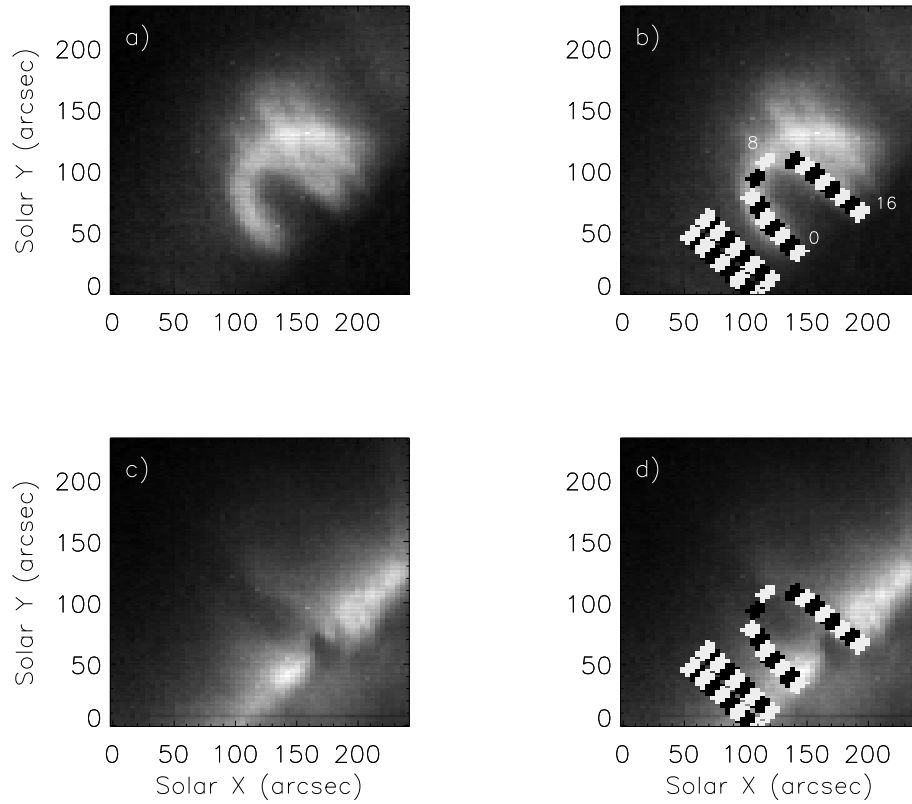


Figure 3. Coronal loop observed in a) Fe XVI 360.7 Å and in c) Si X 347.4. Images b) and d) show an overplot of the selected sections where the N_e has been determined. The two profiles on the left side of images b) and d) were used as a comparison. On image b) the indices of the starting, middle and final section of the loop are overplotted.

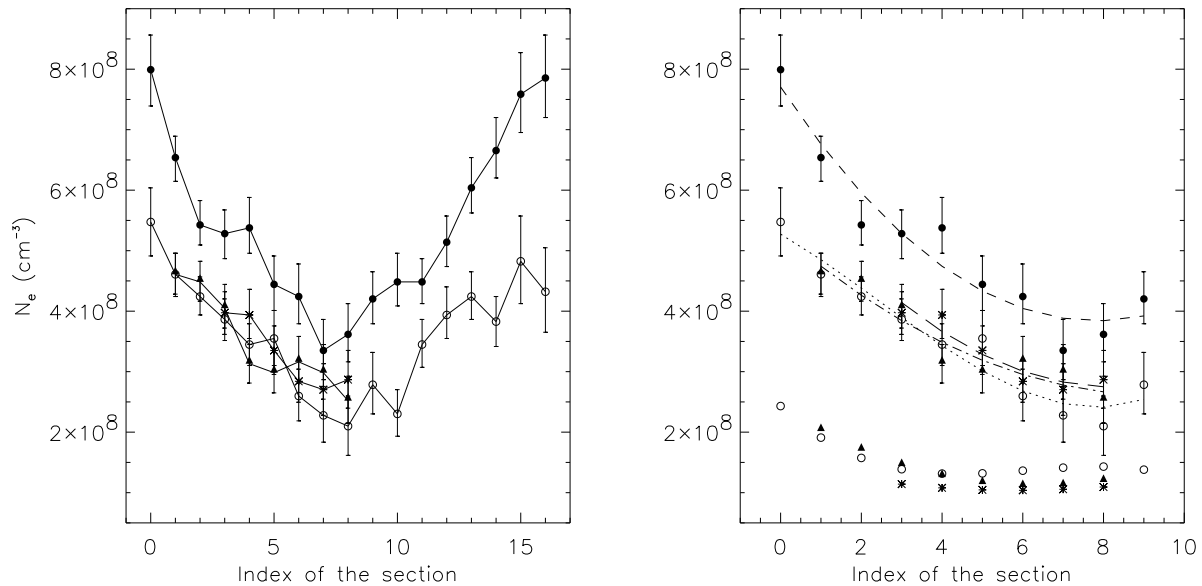


Figure 4. Left: N_e along the loop, black circles; same locations the previous day, open circles; and two radial profiles outside the loop, asterisks and black triangles. Right: same from section 0 to 9. Lines represent polynomial fits to the N_e values: dashed for black circles (order 3), dotted for open circles (3), long dashed for asterisks (2) and dash-dot for black triangles (2). The symbols below represent the difference between the dashed fit and the other three, respectively, i.e the estimated N_e along the loop.

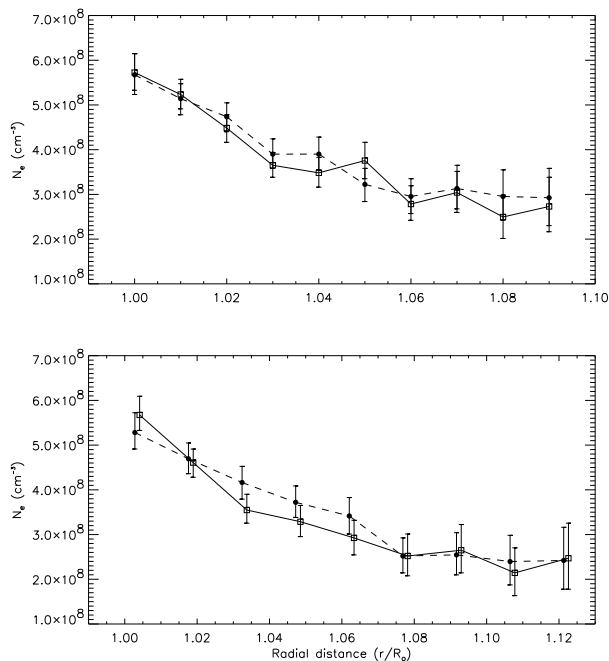


Figure 5. Radial decay off limb of N_e for two successive days. Top: empty squares represent a radial profile of the electron density at 220.5° on March 28 and filled black circles on March 29. Bottom: the same at 59° on April 1 and April 2.

above with a polynomial function. A third degree polynomial was required to fit the values of N_e at sections 0 to 9 along the loop and the same sections the day before (dashed and dotted lines, Figure 4 right). For the other two profiles we used a second degree polynomial. The difference of the fittings gave us an estimation of the behaviour of the electron density along the loop (symbols without bars). Figure 4 left shows all the sections along the loop. In the final results we don't include sections 10 to 16 because of a small feature, probably prominence, overlying the right footpoint.

These results suggest that the loop presents a higher N_e at the footpoints, reaching a value of $\sim 2.5 \times 10^8 \text{ cm}^{-3}$. From section 4 to the apex (7-8) it remains practically constant with a value ranging $\sim 1.0 - 1.5 \times 10^8 \text{ cm}^{-3}$.

At section 7, the value of the loop approaches noticeably the value of the quiet sun (Figure 4), which is not reproduced by the smooth curve of the fit. This confirms the first sight impression that the loop has less emission, proportional to N_e , at the apex for these cooler lines.

CONCLUSIONS

A detailed study of the electron density off limb has been done leading to the expected latitudinal behaviour of electron density increase from the poles to the equator and decrease again towards the pole, but extended to the whole disk. Our intention is to apply into the data the latitudinal model of the solar wind developed by Lima, Priest &

Tsinganos (2001). The temporal variation of N_e in consecutive daily rasters has also been studied, and we have found that the radial decay remains constant from one day to the next, within our error bars which go from 10% near the limb to 40% at 1.09 solar radii. This result gives us an useful tool to study phenomena like the loop found in one of our rasters. Based on the previous result we have found that the footpoints of the loop have higher electron density at this temperature than the rest of it, and that the value becomes constant as we approach to the apex.

ACKNOWLEDGMENTS

Research at Armagh Observatory is grant-aided by the Department of Culture, Arts and Leisure for N. Ireland. This work was partly supported by PPARC grant PPA/G/S/1999/00055. I.U.U. and M.S.M. would like to thank the LOC for the EC grant which made it possible to attend the conference.

REFERENCES

- Gallagher P.T., Mathioudakis M., Keenan F.P., Phillips K.J.H. & Tsinganos K., 1999, ApJ, 524, L133
 Lima J.J.G. & Priest E.R., 1993, A&A, 268, 641
 Lima J.J.G., Priest E.R. & Tsinganos K. 2001, A&A, 371, 240